Structure determination of $Si(100)(2 \times 1)/NH_2$ using scanned-energy mode photoelectron diffraction

1997 J. Phys.: Condens. Matter 9 8419

(http://iopscience.iop.org/0953-8984/9/40/009)

J. Phys.: Condens. Matter **9** (1997) 8419–8432. Printed in the UK PII: S0953-8984(97)85730-X

Structure determination of Si(100)(2 × 1)/NH_2 using scanned-energy mode photoelectron diffraction

N Franco†, J Avila†, M E Davila†, M C Asensio†, D P Woodruff‡, O Schaff§, V Fernandez§, K-M Schindler§ and A M Bradshaw§

† Instituto de Ciencia de Materiales, CSIC, Cantoblanco, 28049 Madrid, Spain
‡ Physics Department, University of Warwick, Coventry CV4 7AL, UK
§ Fritz-Haber-Institut der Max-Planck-Gesellschaft, Faradayweg 4-6, 14195 Berlin, Germany

Received 7 July 1997

Abstract. A scanned-energy mode photoelectron diffraction study of the Si(100)(2 × 1) surface with adsorbed NH_2 has provided quantitative determination of key structural parameters previously only predicted from theoretical calculations. The N atoms are found to occupy off-atop sites at a dimerized surface Si atom with an N–Si bondlength of 1.73 ± 0.03 Å and bond angle relative to the surface normal of $21 \pm 4^\circ$. The positions of Si atoms in the dimer to which the adsorbates are bonded are found to indicate that the marked asymmetry of this dimer on the clean surface is lost as a result of the adsorption. The conclusions are discussed in relation to published results from less direct experimental probes and the results of theoretical model calculations.

1. Introduction

The surface chemistry of Si is of considerable practical interest in the context of semiconductor device processing. Silicon remains the most widely used semiconductor material and its chemistry in the gas phase is relevant to many aspects of the fabrication of a range of different heterojunctions including semiconductor–insulator, semiconductor–metal and semiconductor–semiconductor interfaces. As a result there exists a large body of published work reporting studies of these adsorption systems by a variety of (vibrational, electronic and thermal) spectroscopies and there have also been a large number of related theoretical studies. By contrast there are very few experimentally derived quantitative structural data which can serve as a base on which to develop our understanding of the electronic and geometrical structure and the chemical reactivity. One specific example of such a system is the interaction of Si(100) with NH_3, of potential interest to surface nitridation. Ammonia is found to adsorb dissociatively on Si(100) even at low temperature (90 K) and at room temperature there is general agreement (from electronic and vibrational spectroscopies) that the resulting surface has coadsorbed NH_2 and H [1–8]. An early scanning tunnelling microscopy study at room temperature [9] was interpreted in terms of subsurface atomic N and adsorbed H but the general consensus concerning the probable structure is now of the NH_2 and H species adsorbed at opposite ends of the Si dimers present on the clean surface. This consensus, however, is based only on indirect experimental evidence and theoretical total energy calculations [10, 11], and indeed the fact that the early conclusions have now been modified highlights the ambiguity of interpretation of many of the (essentially electronic) spectroscopic probes.

0953-8984/97/408419+14$19.50

Here we present the results of a quantitative structural study of the $Si(100)/NH_2$ system using the technique of scanned-energy mode photoelectron diffraction (PhD) [12]. This technique exploits the coherent interference of the directly emitted component of the photoelectron wavefield resulting from an adsorbate core level with other components of the same wavefield elastically backscattered from surrounding (mainly substrate) atoms. It provides a rather local structural probe of the environment of the adsorbate emitter; one advantage of this localization for semiconductor surface structure determination is that the information obtained is rather insensitive to multilayer substrate relaxations known to occur at such surfaces. While the structural information obtained may therefore be formally incomplete, it is nevertheless unambiguous. This contrasts with a technique such as low-energy electron diffraction (LEED) in which there is now ample evidence that failure to account for quite subtle substrate modifications can lead to incorrect determinations of more primary adsorbate structural parameters.

Despite the fact that the primary structural information to emerge from our N 1s PhD study is the nearest-neighbour bonding geometry of the N atom—i.e. the N adsorption site and the N–Si bondlength and bond angle—we have also explored the extent to which the presence of the adsorbate modifies the most basic element of the Si(100) clean surface structure, the Si–Si dimer. Although the results are less equivocal in this case there is substantial evidence concerning the modification of this dimer. In this context we should note, however, that the present state of knowledge of the detailed quantitative structure of the clean surface of Si(100) is considerably less clear than one might expect for such a widely studied surface. As this surface is the reference point for any adsorbate-induced surface modification discussion, we devote a short section of this paper to a critical summary of this topic. This is presented in section 3 immediately after the description of the experimental details and the first-order structural results (section 2) and prior to a more detailed quantitative analysis of the PhD data resulting from our experiment.

2. Experimental details and preliminary results

The experiments were conducted at the BESSY synchrotron radiation facility in Berlin using the HE-TGM1 beamline and end-station described elsewhere [19, 20]. This ultra-high-vacuum end-station is equipped with a sample manipulator allowing heating and cooling of the sample as well as the ability to rotate the sample azimuthally about its surface normal and in polar incidence and emission angle by a vertical rotation axis passing through the front face of the sample. *In situ* characterization of the surface order and cleanness was achieved with LEED and with soft-x-ray core level photoemission based on the synchrotron radiation. Sample cleaning was achieved by cycles of argon ion bombardment and heating to 1500 K until a clean (especially carbon-free) surface was obtained which displayed a well ordered two-domain (2×1) LEED pattern. The adsorbate structure was formed by exposing this surface at room temperature to 1 L of NH_3 gas, a procedure widely established to produce a near-saturation coverage of coadsorbed NH_2 and H. A two-domain (2×1) LEED pattern remained after this treatment. The sample was then cooled to 200 K for the PhD measurements in order to achieve some reduction of vibrational amplitudes and associated Debye–Waller factors in the electron interference phenomena.

The scanned-energy mode photoelectron diffraction (PhD) technique [12] involves measurement of the intensity of an adsorbate core level photoemission signal in a specific direction as a function of photoelectron kinetic energy; this intensity is modulated because, as the photoelectron wavelength changes, backscattering pathways become alternately constructive and destructive. A first-order structure analysis can be obtained from a set

of such PhD spectra recorded in different emission angles by a simple Fourier-transform method [13, 14]; the emission directions corresponding to 180° substrate atom backscattering lead to PhD spectra dominated by this one scattering path, so a Fourier transform shows a particularly intense peak at short apparent scattering pathlength difference. In this way the direction of the nearest-neighbour backscatterers, and thus the adsorption site, can be identified. However, this information is only approximate, as the methodology takes no formal account of the role of multiple scattering or scattering phase shifts. A full quantitative analysis is thus also necessary using structural ('trial-and-error') iteration through a comparison of the experimental spectra with the results of multiple-scattering simulations [15–18] for a series of trial structures. In the present case a total of nine N 1s PhD spectra recorded at polar emission angles of 0°, 5°, 10°, 20°, 30° and 40° in a ⟨110⟩ azimuth and of 10°, 20° and 30° in a ⟨100⟩ azimuth, each in the kinetic energy range 45–420 eV, covering a total energy range of 3375 eV, was used in the structure determination. Additional spectra in other emission directions were also collected to check for directions corresponding to strong modulations, and the larger set of 18 spectra were used in the approximate site identification stage using the Fourier transform method. The spectra were collected using a fixed, 152 mm mean-radius spherical-sector electrostatic analyser (VG Scientific) fitted with three channeltrons for three-channel parallel detection. The analyser is installed to collect electrons emitted in the horizontal plane (which also coincides with the plane of incidence and polarization of the photons) and has a fixed angle of 60° relative to the photon incidence. Different polar emission and azimuthal angles were obtained by sample rotation. Each PhD modulation spectrum was obtained by measuring short (30 eV) photoelectron energy spectra around the N 1s peak for a series of photon energies in 2 eV steps in the energy range approximately 440–840 eV. The individual peak areas were then determined as a function of photoelectron energy and normalized to a smooth spline passing though this spectrum to obtain an experimental modulation function.

Fourier transform intensity contour maps obtained from the PhD spectra recorded in the two principal azimuths are shown in figure 1. The dominant peak occurs at an effective scattering pathlength of approximately 3 Å close to normal incidence. Bearing in mind a probable phase shift correction of several tenths of an Å to this pathlength, this suggests that the Si nearest neighbours to the N emitters lie directly below, and thus that the N atoms occupy sites approximately atop surface Si atoms. Note that because of the effective fourfold rotational symmetry of the LEED pattern, the PhD information for any off-atop geometry must average over at least four inequivalent domains (more if the mirror symmetry is broken), so one can anticipate that these Fourier transform maps could be compatible with a range of adsorption sites reasonably close to atop (i.e. the Si–N bond need not be exactly perpendicular to the surface). Nevertheless, the approximate atop site is consistent with previous assumptions that the NH_2 species bonds to one end of the surface Si dimers.

3. The Si(100)(2 × 1) clean surface structure

Despite the fact that the Si(100)(2 × 1) clean surface phase has been recognized for more than 30 years [21] and that quantitative LEED data for the system were published 20 years ago [22], a reliable quantitative structure determination for this system has been slow to emerge. The reason for this was hinted at even in this very earliest qualitative LEED work [21] which showed evidence for some quarter-order diffraction beams under certain conditions, and it now seems well established that at low temperatures a fully ordered surface does show a larger surface net (typically c(4 × 2) but (2 × 2) and c(4 × 4) are also cited). Even in these early studies the common idea was that the basic structural element of all of

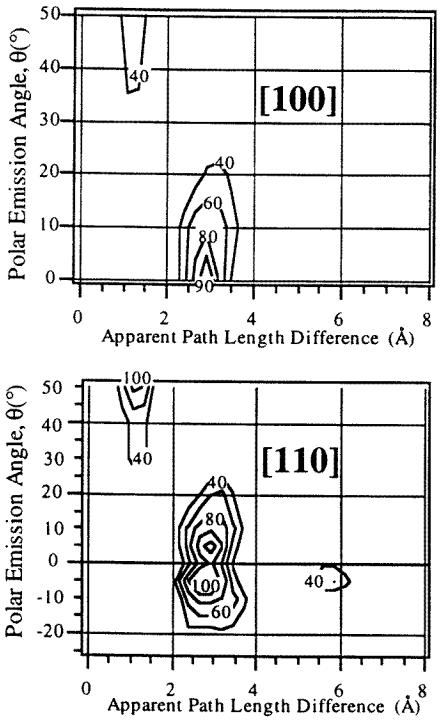

Figure 1. Fourier transform intensity contour maps obtained from the experimental N 1s photoelectron diffraction spectra in the two principal azimuths.

these surfaces was an Si dimer, while the possibility of an asymmetric dimer means that different dimer ordering may lead to different surface nets. It now seems widely accepted that this is the case, although convincing quantitative evidence has been slow to emerge from both experimental and theoretical studies.

One key complication in determining the Si(100)(2×1) clean surface structure which bears particularly on experimental investigations is the fact that the asymmetric dimers on the surface do not have a static long-range order in this room-temperature phase. This aspect of the problem helped to fuel many of the arguments concerning the symmetry or asymmetry of the dimers. The fact that most scanning tunnelling microscope (STM) studies showed what appeared to be symmetric dimers [23–25] was widely cited as evidence for an absence of significant asymmetry. By contrast, Si core level photoemission spectra show at least two distinct surface-shifted components which have been widely regarded as being associated with emission from the 'up' and 'down' Si atoms of surface asymmetric dimers [26–32] (although the correct assignment of the different chemically shifted peaks has only recently been reliably resolved [33, 34]). It now seems to be accepted that the solution to this apparent dilemma is that at room temperature the asymmetric dimers can 'flip' so that up and down atoms are constantly switching, at a rate estimated to be of order 10^9 s^{-1} [35]. Under these circumstances photoemission, which is several orders of magnitude faster than this flip period, samples the atoms in their 'frozen' up and down positions; STM, on the other hand, samples on a much longer timescale and thus simply averages over many such flips. STM measurements taken at low temperature, which 'freezes out' the dimer flipping, confirm this idea [36].

Having recognized this aspect of the problem, all experimental determinations of the structure of the (2 × 1) phase (which has (2 × 1) ordering of dimers but instantaneous disorder of the dimer asymmetries—i.e. it does not possess true long-range order) need to be evaluated carefully to establish the time-scale of the probe and the nature of the order probed. LEED, for example, relies on true long-range order. Analysis based on single domains of long-range-ordered asymmetric dimers, then averaged (incoherently) over inequivalent domains, will not lead to the same results as attempting to include the variations in local coherence between asymmetric dimers which are randomly ordered. As all current LEED analyses [37, 38] are based on the former approach, the local dimer geometries obtained may well be in error. A similar problem exists for surface x-ray diffraction (SXRD), with the exception that a value of the height difference between the up and down ends of the dimers obtained from analysis of a (00) beam reciprocal lattice rod scan does not rely on long-range lateral order and so should still yield a reliable value. Local techniques not reliant on long-range order (e.g. ion scattering or photoelectron diffraction) are not troubled in this way, and are all based on interaction times short enough to detect the instantaneous dimer geometry between flips. Nevertheless, such methods will provide information which averages over the two different flipped orientations. If these considerations are used to filter the published structural studies one finds that the most direct and potentially reliable experimental determinations of the dimer asymmetry are rather consistent. Dimer bond angles relative to the surface plane are 14° based on medium-energy ion scattering [39], 20° from a specular beam SXRD rod scan [40], and 19° from a forward-scattering x-ray photoelectron diffraction (XPD) study [41]. Smaller values from an earlier SXRD study (7.4°) [42] and a transmission electron diffraction investigation (6.8°) [43] are both obtained indirectly from in-plane projections of the structure combined with assumed bond lengths. Lower values from LEED studies are also ignored for the reasons given above.

There have also been many attempts to determine the optimum surface geometry from theoretical total-energy calculations. Most of the early work of this kind failed to detect any preference for dimer asymmetry, but all of the most recent and most sophisticated calculations do show the asymmetric dimer to be favoured with dimer tilt angles similar to those cited above as being the most reliable experimental values. For example, two recent local density-functional calculations gave values of 15° [35] and 17° [44]; a very recent tabulation of such theoretical calculations shows values mainly in the range 15° to 19° [45]. The best current information, therefore, indicates that the clean Si(100) surface comprises asymmetric dimers with a dimer bond angle relative to the surface plane which lies in the range $17 \pm 3°$. All the more recent theoretical calculations yield Si–Si dimer bondlengths within ±0.02 Å of a value of 2.27 Å; the scatter of the experimental values is much larger (up to ±0.20 Å) but many of these values are subject to doubt for the reasons discussed above.

4. Full structure analysis for Si(100)(2 × 1)/NH$_2$

In order to obtain a full quantitative structure determination using the PhD data, the experimental spectra are compared with the results of full multiple-scattering calculations for a series of trial structures, concentrating on geometries involving the N emitter in a near-atop site as indicated by the Fourier transform maps. As we have already remarked, a potential complication in determining semiconductor surface structures is the likelihood that there may be significant distortions in bond angles and bond lengths relative to the bulk values several layers down below the surface. This means that there may be a very large number of structural variables (the coordinates of many layers of Si atoms). However,

the PhD technique is essentially a local structural probe, most sensitive to the locations of the backscatterer substrate atoms relatively close to the adsorbate emitter, and rather insensitive to movements of more distant scatterers. For this reason the computational results presented here concentrate on models in which most of the substrate atom relative positions were constrained to bulk values. Calculations made to investigate the possibility of deeper-layer substrate distortions confirmed the insensitivity of the data to such an effect and showed, as a consequence, that the precision with which such unconstrained coordinates could be found was very low (up to several tenths of an ångstrom).

Our structural optimization using full multiple-scattering simulations [15–17] of the complete photoelectron diffraction data set described above were conducted with the aid of a 'linear' approximation method [18] to allow multiple-parameter scans of the structural parameter space, and automated optimization of multiple parameters using exact calculations and a Newton–Gauss optimization procedure. The optimization was achieved through minimization of a reliability factor (*R*-factor) [46] based on a sum of square deviations between theory and experiment normalized in a similar fashion to the Pendry *R*-factor [46] used in quantitative LEED. The precision was estimated using a variance also computed as described by Pendry [47].

The structural parameters to which the photoelectron diffraction data are most sensitive locate, relative to the N emitter, the surface Si atom to which the N atom in the NH_2 species is bonded; this defines the Si–N bondlength and bond angle relative to the surface. In addition, of course, the data show some sensitivity to the location of the N emitter and its Si nearest neighbour relative to the remainder of the Si substrate. Of especial interest in this context is the degree of asymmetry of the Si dimer to which the NH_2 is bonded. For this reason the constrained searches concentrated on moving the N emitter and each of the two nearest-neighbour Si surface dimer atoms to which the N is bonded both relative to each other and relative to an underlying ideally terminated bulk Si substrate. Freeing other structural parameters led to wholly insignificant improvements in the *R*-factor. Figure 2 shows plan and sectional views of the model structure and labels the atoms; this figure thus defines the structural parameters investigated, namely the coordinates of each of the N (labelled N) and surface Si dimer atoms (S1 and S2) relative to the underlying ideally terminated bulk Si(100) substrate. The coordinate system used has x along [110] and z along the surface normal [001]. Our notation is that x_{13}, for example, is the x coordinate of S1 relative to S3, while the bondlength between these two atoms would be labelled ρ_{13}. Only two bond angles are discussed, the N–Si nearest-neighbour bond angle θ_{N1}, which is defined relative to the surface normal, and the Si dimer bond angle Θ_{12}, which is defined relative to the surface plane.

The key finding of our structure determination is that the NH_2 does, indeed, bond to a surface Si atom in a location consistent with attachment to the dimer dangling bond. Figure 3 shows a comparison of the best-fit theoretical calculations and the experimental photoelectron diffraction spectra. The structural parameters corresponding to this best-fit model are summarized in table 1, while figures 4–6 show the variation of the *R*-factor as a result of changes in the various structural parameters in the vicinity of the best fits; these figures are discussed in more detail below. The low overall *R*-factor value of 0.165 is consistent with the excellent fit of all major features, and the variance was estimated to be 0.011, so the range of parameter values defining the error estimates corresponds to fits leading to *R*-factors below 0.176 (R_{min} plus this variance). As figure 4 shows, the *R*-factor is very sensitive to movements of the N emitter atom relative to the nearest-neighbour Si atom. The determined Si–N bond angle relative to the surface normal ($21 \pm 4^\circ$) and bondlength (1.73 ± 0.03 Å) are in good agreement with the values of these parameters (22.8° and

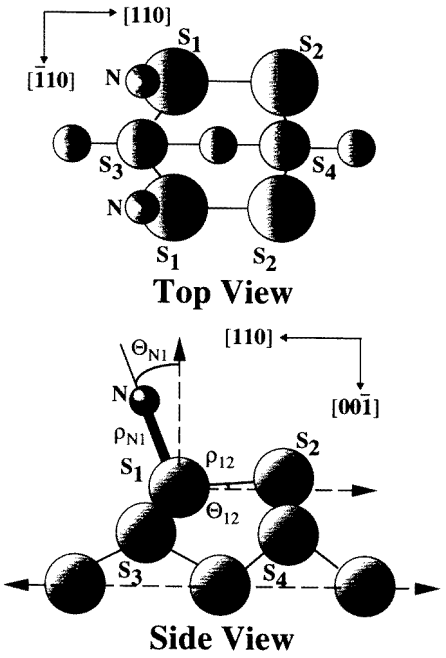

Figure 2. Schematic diagram showing the optimized structure for the N atom in adsorbed NH_2 on Si(100) obtained from fitting the N 1s photoelectron diffraction data by multiple-scattering calculations. The labelling convention for the different surface atoms and for bondlengths and bond angles is as used in the text.

Table 1. Summary of the main structural parameter values obtained in this analysis, using the labelling of figure 2. For the values bracketed the (very poor) precision estimates are approximate only, as discussed in the text.

x_{N1}	-0.63 ± 0.06 Å
z_{N1}	1.61 ± 0.02 Å
ρ_{N1}	1.73 ± 0.03 Å
Θ_{N1}	$21 \pm 4^\circ$
x_{13}	0.50 ± 0.25 Å
z_{13}	1.12 ± 0.06 Å
x_{23}	$(3.3 \pm 0.3/-0.6$ Å)
z_{23}	$(1.5 \pm 0.4$ Å)
ρ_{12}	$(2.8 \pm 0.3/-0.6$ Å)
Θ_{12}	$(8 \pm 8^\circ)$

1.707 Å respectively) of the published slab calculations [11]; by contrast, while the cluster calculation gave a similar bond angle (25°) the bondlength deduced in this calculation (2.04 Å) lies well outside the estimated errors of the experimental determination. The only other estimates of the Si–N bond angle to be found in the published literature are somewhat speculative in their basis; our value is consistent with the estimate of 20° made by Fujisawa *et al* [7] but not with the 35° estimated by Dresser *et al* [8].

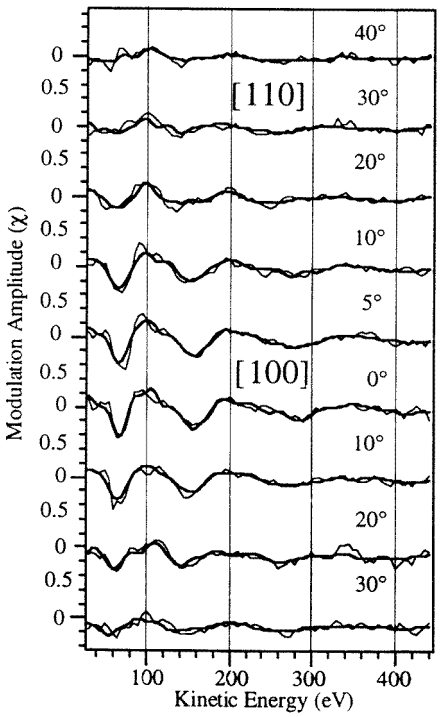

Figure 3. Comparison of experimental N 1s photoelectron diffraction spectra (thin lines showing experimental noise) from NH_2 on Si(100) with the results of multiple-scattering calculations (thick lines) for the best-fit structure.

The key additional information we seek concerns the degree of asymmetry of the Si dimer to which the NH_2 is bonded. This may be established in two possible ways. Firstly, if the location of the S2 Si atom which forms the other half of the dimer to which the NH_2 is bonded can be established, one can determine the S1–S2 dimer bond angle relative to the surface. Alternatively, or additionally, one can locate the S1 Si atom to which the NH_2 is bonded, relative to the substrate; dimer asymmetry leads to a significant change in the location of the dimer atoms both parallel and perpendicular to the surface relative to the underlying substrate.

As may be expected, the sensitivity of the results to the location of the Si atom at the other end of the dimer, S2, which is not involved in bonding to the NH_2, is poor. This single Si atom falls into the favoured backscattering geometry relative to the N emitter only at angles well removed from normal emission, where averaging over the four locally inequivalent domains further reduces the contribution of this scatterer. As may be seen from the *R*-factor contour map of figure 5, which shows the sensitivity of the PhD fits to the location of the S2 atom (all other atomic positions being held constant), the minimum is a very shallow one. The actual location of this minimum corresponds to an Si–Si dimer bondlength of 2.8 Å, but with very poor precision (probably worse than ± 0.7 Å—figure 5 does not extend far enough to fix these values), while the dimer bond angle value relative to the surface plane is found to be 8° with an error estimate of at least $\pm 8^\circ$. This dimer bond angle covers the range corresponding to both a perfectly symmetric dimer (0°) and one having the full asymmetry of the clean surface (around 15° as discussed in the previous

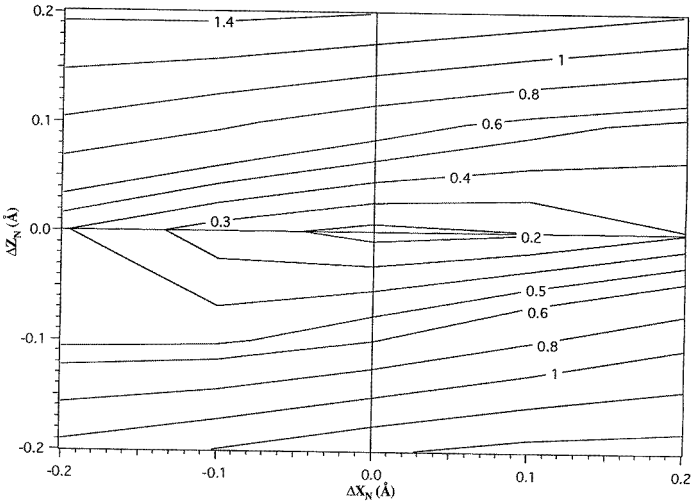

Figure 4. *R*-factor contour map showing the dependence of the PhD theory–experiment fit on the location of the N emitter atom relative to the S1 nearest-neighbour Si dimer atom. The axes (Δx_N and Δz_N) are the positions relative to the optimum position as given in table 1. As discussed in the text, acceptable fits to the experimental data for this system correspond to those structures yielding an *R*-factor $\leqslant 0.176$. In this figure such a contour would lie inside the region defined by the contour corresponding to a value of 0.2 (the centre of this map corresponds to the best-fit *R*-factor value of 0.165).

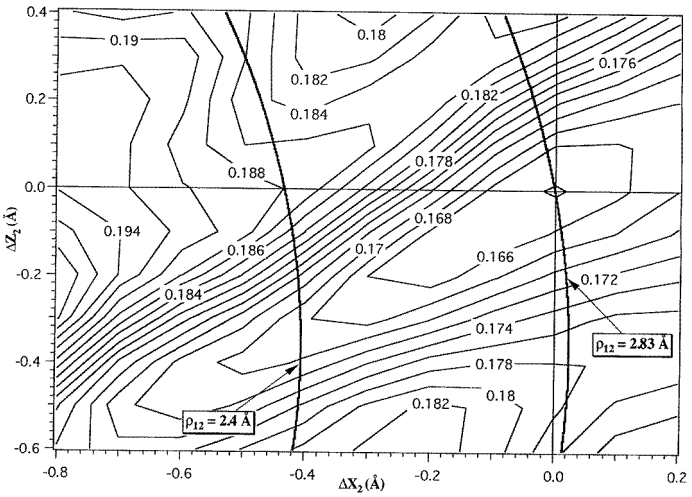

Figure 5. *R*-factor contour map showing the dependence of the PhD theory–experiment fit on the location of the S2 Si dimer atom (Δx_2 and Δz_2) relative to its optimum position as given in table 1. For the purposes of calculating this contour map the location of the emitter (N), nearest-neighbour Si atom (S1) and all other Si atoms were held fixed. Also shown are lines of constant values of ρ_{12} corresponding to 2.83 Å (the best-fit value at the minimum on the map) and 2.40 Å (a value more typical of that expected). Structures falling within the $R = 0.176$ contour are all deemed to be acceptable as discussed in the text.

section). The 'best' value of the dimer bondlength is almost certainly too large, but in view of the poor precision the result is also consistent with typical values from theory (the slab

calculations for the Si(100)/NH_2 system [11] give a value of 2.42 Å). Despite the huge ambiguity in the S2 atom position, figure 5 shows that there is clearly some coupling of the x and z coordinates of this atom as the R-factor minimum is elongated along a diagonal line of this map. Interestingly, if one adds the locus of points of constant S1–S2 dimer bondlength to this map, these lines run almost directly perpendicular to the R-factor valley. In effect this shows that the sensitivity of the PhD data is much higher to the dimer bond angle than to the dimer bondlength. Much of the reason for this is related to the fact that the data are most sensitive to the distance of the S2 atom from the emitter, N. A line of constant ρ_{N2} more nearly runs along the shallow valley. The dominant sensitivity of PhD to emitter scatterer bondlengths and the resulting parameter coupling has been observed in previous systems and discussed in greater depth [48, 49].

In view of the fact that we expect the Si–Si dimer bondlength to be significantly less than 2.8 Å, it is instructive to consider briefly the consequences of constraining this parameter to a more reasonable value of approximately 2.4 Å. A line corresponding to this value is shown on figure 5. Notice that this now crosses the R-factor valley minimum at a significantly (approximately 0.37 Å) lower value of the z coordinate of the S2 atom; indeed, this forced lowering of S2 is such as to make the optimum (constrained) fit correspond to a dimer exactly parallel to the surface within the limits of precision; this constrained fit leads to a dimer bond angle, Θ_{12}, of $0 \pm 8^\circ$. This value for the dimer bond angle is significantly different from the clean surface dimer asymmetry, and indicates an essentially symmetric dimer in the presence of the adsorbed ammonia products. The fact that this conclusion is based on a fit constrained away from the true R-factor minimum for the PhD data means, however, that it cannot be seen as a wholly convincing case for ammonia-induced dimer restructuring.

A far more conclusive indicator of the dimer asymmetry emerges from a determination of the location of the S1 Si atom relative to the substrate. The Si–Si dimer asymmetry not only leads to a dimer axis rotation but also has an associated displacement of the dimer centre parallel to the surface along the dimer direction, while the dimer rotation itself causes a significant change in the layer spacings of both dimer atoms relative to the second Si layer. These displacements are quite large; for example, if we compare the calculated coordinates given for a symmetric dimer [50] and an asymmetric dimer [44], the 'down' atom is displaced perpendicular to the surface (down) by 0.34 Å and parallel to the surface by 0.24 Å; the comparable figures for the 'up' atom are 0.36 Å (up) and 0.19 Å (see table 2). We see, therefore, that alternative information on the likely level of asymmetry of the Si dimer can be obtained from the location of the S1 atom relative to the substrate; this parameter should be obtainable with significantly higher precision than any attempt to determine the position of S2. This expectation is confirmed by the R-factor map of figure 6. Because the dominant scattering contributing to the PhD spectra arises from the S1 nearest-neighbour Si scatterer to the N emitter, the sensitivity to the position of S1 relative to the substrate must be obtained by moving *both* the N emitter and S1 scatterer together (moving the S1 atom alone determines mainly the sensitivity to the N–Si bondlength and bond angle). As expected, figure 6 shows a strong sensitivity to the height of the emitter and S1 relative to the substrate, and substantially lower sensitivity to the positions parallel to the surface (although this sensitivity is still very significantly higher than for the S2 atom position seen in figure 5).

The potential relevance of the location of the S1 atom to the question of dimer asymmetry is shown in table 2 in which the measured locations of the S1 and S2 dimer atoms relative to the substrate are compared with predictions for the clean surface based on ideal (1×1) bulk termination and on symmetric and asymmetric dimers. Notice that on the

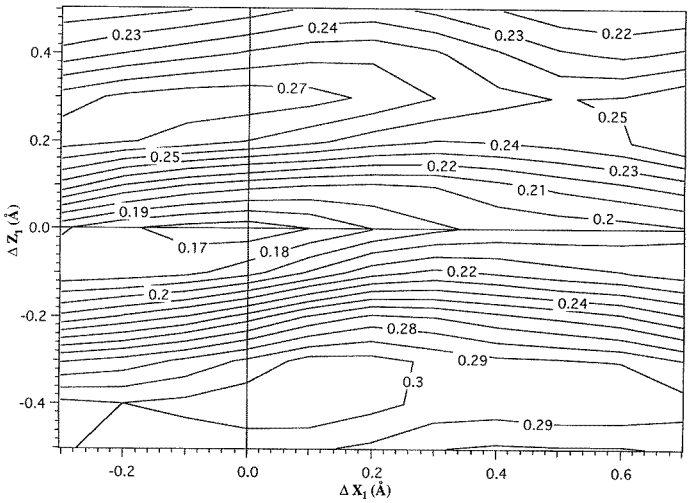

Figure 6. *R*-factor contour map showing the dependence of the PhD theory–experiment fit on the location of the S1 Si dimer atom relative to its optimum position as given in table 1. For the purposes of calculating this contour map the location of the emitter (N) and the nearest-neighbour Si atom (S1) have been moved together relative to all other Si atoms as described in the text.

Table 2. Comparison of surface dimer atom positions (in Å) obtained in the present study of the NH_2/H coadsorption system and for the clean Si(100) surface assuming ideal bulk (1 × 1) termination, a (2×1) symmetric dimer structure [50], or a (2×1) structure comprising asymmetric dimers as calculated for a c(4 × 2) phase [44].

	Clean Si(100)				
	Ideal bulk (1 × 1)	Symmetric dimer	Asymmetric dimer		Si(100)/NH_2/H (this work)
			S1 down	S1 up	
x_{13}	0.00	0.80	1.04	0.61	0.50 ± 0.25
z_{13}	1.36	1.03	0.69	1.39	1.12 ± 0.06
x_{23}	3.84	3.04	3.23	2.80	$(3.3 + 0.3/-0.6)$
z_{23}	1.36	1.03	1.39	0.69	(1.5 ± 0.4)

clean surface the dimer bondlength ρ_{12} is only 2.24 Å, smaller than expected after the NH_2 adsorption. This comparison shows rather clearly that while the low precision of the S2 atom coordinates prevents us clearly distinguishing the symmetric and asymmetric dimer geometries without constraining the dimer bondlength, the coordinates of S1 are much more consistent with a near-symmetric dimer than with the level of asymmetry characteristic of the clean surface. This statement is clearly true for the lateral position (x-coordinate) of the Si near-neighbour dimer atom but is even clearer for the substrate layer spacing z-coordinate. This parameter is clearly inconsistent with either the up or down atom of the asymmetric dimer (i.e. reversing S1 and S2, as shown in the second column of the theoretical values for the asymmetric dimer in table 2, does not improve the agreement between our experimental value and those of the clean surface asymmetric dimer). Strictly, of course, table 2 also indicates disagreement between the S1–S3 layer spacing, z_{13} (1.12 ± 0.06 Å) and the calculated value for a symmetric clean surface dimer (1.03 Å). On the other hand, we note that it is now acknowledged that the clean surface dimer is *not symmetric*, so this

calculation should be regarded as indicative of the kind of value which would accompany a symmetric clean surface dimer, rather than a formal expectation for our adsorbate system. Indeed, one expects the presence of the adsorbed NH_2 and H to have some effect on all the Si surface coordinates (especially the dimer bondlength) relative to the clean surface. In particular, if we increase the Si dimer bondlength ρ_{12} to 2.42 Å [11] for the symmetric dimer geometry of table 2, simple geometry (keeping other bondlengths fixed and retaining subsurface atom locations) yields a reduction of x_{13} to 0.71 Å and an increase in z_{13} to 1.09 Å, both in agreement with our experimental values. The slab calculation which includes these adsorbates [11] actually yields a value for z_{13} of 1.19 Å, very close to the measured value albeit slightly *larger*. This same calculation gives an optimum value of 2.2° for the dimer bond angle, a value consistent with an essentially symmetric configuration. The experimental coordinates of the S1 Si dimer atom are consistent with a geometry very close to symmetric, and inconsistent with an asymmetry as large as that of the clean surface.

5. Discussion and conclusions

The only other experimental evidence germane to the dimer asymmetry arises from measurements of Si 2p photoemission core level binding energy shifts. Changes in the values seen on the clean surface associated with NH_2/H coadsorption have been reported and can be interpreted in terms of a greater covalency and thus reduced asymmetry [51]. Within this type of description the difference in Si 2p binding energies between the up and down atoms of the clean surface asymmetric dimer is assigned to charge transfer within the dimer and thus to ionicity in this bond. Such arguments, however, are based only on initial-state energy changes and ignore the role of final-state relaxation. On the other hand, it is notable that the full calculation of the surface binding energy shifts for the clean surface [35] does attribute the additional screening effects to the presence of occupied and unoccupied dangling bond states on the two ends of the dimer, also consistent with the existence of significant charge transfer. Of course, the complicating presence of the chemisorbed NH_2/H coadsorbates restores the ambiguity of interpretation of the surface core level shifts in terms of geometric dimer asymmetry.

One interesting analogue to this system is the behaviour of III–V(110) semiconductor surfaces. The ideally terminated form of these surfaces would have coplanar anions and cations, but the stable structures involve rotation of this bond angle to produce a situation akin to that of the Si asymmetric dimers; a key difference, of course, is that on the III–V surfaces the ideal unreconstructed surface already has local positive and negative charges on the elementally inequivalent atoms, whereas on Si(100) the charge redistribution and local ionicity is only present after the relaxation. One example of an adsorption structure which has been solved on such a surface concerns H_2S interaction with InP(110), believed to lead to coadsorbed SH and H. In this system a structural study using x-ray standing waves [52] shows that such adsorption causes the clean surface bond rotation to be removed, restoring a bulk-terminated surface below the adsorbate.

In summary, we have used scanned-energy mode photoelectron diffraction to provide the first quantitative determination of a molecular adsorbate geometry on a technically important Si surface, specifically coadsorbed NH_2 and H on Si(100) resulting from interaction with NH_3. The results confirm prior speculation concerning the adsorption sites, and provide quantitative structural parameters in good agreement with one of the previous theoretical calculations on this system. The results not only provide quantitative values for the Si–N bondlength and bond angle, but also show that the adsorbates substantially reduce, or possibly remove, the geometrical asymmetry of the Si dimers present on the clean surface.

Acknowledgments

The authors are pleased to acknowledge the financial support of this work in the form of grants from the DGICYT (No PB-94-0022-C02-01), the Engineering and Physical Science Research Council (UK), the European Community through the Human Capital and Mobility Networks (grant No ERBCHRXCT930358) and Large Scale Facilities programmes, and the German Federal Ministry of Education, Science, Research and Technology (BMBF) under contract number 05 625EBA 6. They also thank Dr Volker Fritzsche for the provision of the multiple-scattering analysis codes and assistance in the installation of these.

References

[1] Bozso F and Avouris Ph 1986 *Phys. Rev. Lett.* **57** 1185
[2] Hill E K, Kubler L, Bischoff J L and Bolmont D 1987 *Phys. Rev.* B **35** 5913
[3] Bozso F and Avouris Ph 1988 *Phys. Rev.* B **38** 3937
[4] Kubler L, Bischoff J L and Bolmont D 1988 *Phys. Rev.* B **38** 13 113
[5] Bischoff J L, Lutz F, Bolmont D and Kubler L 1991 *Surf. Sci.* **251/252** 170
[6] Bischoff J L, Kubler L, Bolmont D, Sébenne C A, Lacharme J-P, Bonnet J E and Hricovni K 1993 *Surf. Sci.* **293** 35
[7] Fujisawa M, Taguchi Y, Kuwahara Y, Onchi M and Nishijima M 1989 *Phys. Rev.* B **39** 12 918
[8] Dresser M J, Taylor P A, Wallace R M, Choyke W J and Yates J T Jr 1989 *Surf. Sci.* **218** 75
[9] Hamers R J, Avouris Ph and Bozso F 1987 *Phys. Rev. Lett.* **59** 2071
[10] Zhou Ru-Hong, Cao Pei-Lin and Fu Song-Bao 1991 *Surf. Sci.* **249** 129
[11] Moriarty N W and Smith P V 1992 *Surf. Sci.* **265** 168
[12] Woodruff D P and Bradshaw A M 1994 *Rep. Prog. Phys.* **57** 1029
[13] Fritzsche V and Woodruff D P 1992 *Phys. Rev.* B **46** 16 128
[14] Schindler K-M, Hofmann Ph, Fritzsche V, Bao S, Kulkarni S, Bradshaw A M and Woodruff D P 1993 *Phys. Rev. Lett.* **71** 2054
[15] Fritzsche V 1990 *J. Phys.: Condens. Matter* **2** 9735
[16] Fritzsche V 1992 *J. Electron. Spectrosc. Relat. Phenom.* **58** 299
[17] Fritzsche V 1992 *Surf. Sci.* **265** 187
[18] Fritzsche V and Pendry J B 1993 *Phys. Rev.* B **48** 9054
[19] Dietz E, Braun W, Bradshaw A M and Johnson R L 1985 *Nucl. Instrum. Methods* A **239** 359
[20] See e.g. Hofmann Ph, Schindler K-M, Bao S, Fritzsche V, Ricken D E, Bradshaw A M and Woodruff D P 1994 *Surf. Sci.* **304** 74
[21] Lander J J and Morrison J 1962 *J. Chem. Phys.* **87** 729
[22] Ignatiev A, Jona F, Debe M, Johnson D E, White S J and Woodruff D P 1977 *J. Phys. C: Solid State Phys.* **10** 1109
[23] Tromp R M, Hamers R J and Demuth J E 1985 *Phys. Rev. Lett.* **55** 1303
[24] Hamers R J, Tromp R M and Demuth J E 1986 *Phys. Rev.* B **34** 5343
[25] Hamers R J and Köhler U K 1989 *J. Vac. Sci. Technol.* A **7** 2854
[26] Himpsel F J, McFeely F R, Taleb-Ibrahimi A, Yarmoff J A and Hollinger G 1988 *Phys. Rev.* B **38** 6084
[27] McGrath R, Cimino R, Braun W, Thornton G and McGovern I T 1988 *Vacuum* **38** 251
[28] Wertheim G K, Riffe D M, Rowe J E and Citrin P H 1991 *Phys. Rev. Lett.* **67** 120
[29] Lin D-S, Miller T and Chiang T-C 1991 *Phys. Rev. Lett.* **67** 2187
[30] Rowe J E and Wertheim J K 1992 *Phys. Rev. Lett.* **69** 550
[31] Himpsel F J 1992 *Phys. Rev. Lett.* **69** 551
[32] Lin D-S, Miller T and Chiang T-C 1992 *Phys. Rev. Lett.* **69** 552
[33] Pehlke E and Scheffler M 1993 *Phys. Rev. Lett.* **71** 2338
[34] Landemark E, Karlsson C J, Chao Y-C and Uhberg R I G 1992 *Phys. Rev. Lett.* **69** 1588
[35] Dabrowski J and Scheffler M 1992 *Appl. Surf. Sci.* **56–58** 15
[36] Wolkow R A 1992 *Phys. Rev. Lett.* **68** 2636
[37] Yang W S, Jona F and Marcus P M 1983 *Phys. Rev.* B **28** 2049
[38] Holland B W, Duke B B and Paton A 1984 *Surf. Sci.* **140** L269
[39] Tromp R M, Smeenk R G, Saris F W and Chadhi D J 1983 *Surf. Sci.* **133** 137
[40] Takahasi M, Nakatanai S, ItoY, Takahasi T, Zhang X W and Ando M 1995 *Surf. Sci.* **338** L846

[41] Bullock E L, Gunnella R, Pathey L, Abukawa T, Kono S, Natoli C R and Johansson L S O 1995 *Phys. Rev. Lett.* **74** 2756
[42] Jedrecy N, Sauvage-Simkin M, Pinchaux R, Massies J, Greiser N and Etgens V H 1990 *Surf. Sci.* **230** 197
[43] Jayaram G, Xu P and Marks L D 1993 *Phys. Rev. Lett.* **71** 3489
[44] Northrup J E 1993 *Phys. Rev.* B **47** 10 032
[45] Jenkins S J and Srivastava G P 1996 *J. Phys.: Condens. Matter* **8** 6641
[46] Dippel R, Weiss K-U, Schindler K-M, Gardner P, Fritzsche V, Bradshaw A M, Asensio M C, Hu X M, Woodruff D P and González-Elipe A R 1992 *Chem. Phys. Lett.* **199** 625
[47] Pendry J B 1980 *J. Phys. C: Solid State Phys.* **13** 937
[48] Schaff O, Hess G, Fernandez V, Schindler K-M, Theobald A, Hofmann Ph, Bradshaw A M, Fritzsche V, Davis R and Woodruff D P 1995 *J. Electron Spectrosc. Relat. Phenom.* **75** 117–28
[49] Davila M E, Asensio M C, Woodruff D P, Schindler K-M, Schaff O, Weiss K-U, Fritzsche V and Bradshaw A M 1996 *Surf. Sci.* **359** 185–97
[50] Payne M C, Roberts N, Needs R J, Needels M and Joannopoulos J D 1989 *Surf. Sci.* **211/212** 1
[51] Larsson C U S, Andersson C B M, Prince N P and Flodström A S 1992 *Surf. Sci.* **271** 349
[52] Dudzik E, Leslie A, O'Toole E, McGovern I T, Patchett A, Zahn D R T, Lüdecke J, Woodruff D P and Cowie B C C 1996 *J. Phys.: Condens. Matter* **8** 15–24